Desorption-induced structural changes of metal/Si(111) surfaces: Kinetic Monte Carlo simulations

Pavel Kocán,* Pavel Sobotík, and Ivan Ošt'ádal
Charles University in Prague, Faculty of Mathematics and Physics, Department of Surface and Plasma Science, V Holešovičkách 2, 180 00 Prague 8, Czech Republic
(Received 29 May 2013; published 14 August 2013)

We used a configuration-based kinetic Monte Carlo model to explain important features related to formation of the $(\sqrt{3}\times\sqrt{3})R30^\circ$ mosaic of metal and semiconductor atoms on the Si(111) surface. Using first-order desorption processes, we simulate the surprising zero-order desorption spectra, reported in some cases of metal desorption from the Si(111) surface. We show that the mechanism responsible for the zerolike order of desorption is the enhanced desorption from disordered areas. Formation of the $\sqrt{3}\times\sqrt{3}$ mosaic with properties of a strongly frustrated antiferromagnetic Ising model is simulated by a configuration-sensitive desorption. For substitution of desorbed metal atoms by Si adatoms, fast diffusion of the adatoms on top of a 1×1 layer is proposed as the most probable. Simulations of desorption-induced structural transitions provide us a link between underlying atomistic processes and the observed evolving morphologies with resultant macroscopic desorption fluxes. An effect of the desorption sensitivity on a configuration of neighboring atoms is emphasized.

DOI: 10.1103/PhysRevE.88.022403 PACS number(s): 81.15.Aa, 68.35.bg, 68.55.ag, 64.60.De

I. INTRODUCTION

Deposition of metals on the Si(111) surface together with an appropriate thermal activation results in re-organizing of surface atoms to a variety of ordered structures, often with interesting properties. Special attention has been paid to mosaic phases of two-dimensional (2D) alloys with $(\sqrt{3}\times\sqrt{3})R30^\circ$ symmetry (hereafter denoted as $\sqrt{3}\times\sqrt{3}$ for simplicity). These structures are usually induced by desorption of metal atoms (Pb [1–3], Sn [4,5], Tl [6,7]) together with their substitution by Si atoms.

A significant amount of experimental work published on the topic can be divided into two categories. First, studies concerning flux of desorbing atoms, represented mostly by the thermal desorption spectroscopy (TDS), and second, studies focused on the morphology of resultant structures mostly by means of the scanning tunneling microscopy (STM) and the low energy electron diffraction (LEED).

A surprising feature observed repeatedly when monitoring a flux of some metal atoms desorbing from semiconductor surfaces was a zero-order desorption (ZOD) [1,8–12], meaning in general that the desorption flux is not dependent on the surface coverage of desorbing particles. Usually the ZOD indicates the existence of a 2D gaseous phase (in equilibrium with the solid phase) from which the desorption is activated [13], or desorption from defect sites with constant concentration and accessed via fast diffusion. However, in the case of metal desorption from the Si(111) surface, none of the explanations seems to be valid.

Structural properties of mosaic phases and their formation have been studied both theoretically by *ab initio* and Monte Carlo methods and experimentally using STM and LEED. The experimentally obtained locally ordered mosaic phases have been explained as a result of a repulsive interaction of the same-element nearest neighbors [2,5]. Such situation is an analog of a two-dimensional antiferromagnetic Ising model in a hexagonal lattice, which is strongly influenced by a geometrical frustration of the system. Even though the mosaic phases are usually prepared by a desorption from phases with higher coverages of metal atoms, the relation of the mosaic phase formation to the desorption processes has not been addressed so far.

In this paper, we study a desorption-induced evolution of Pb and Tl structures on Si(111) surface, representing model examples sufficient to study general phenomena of the transition from the (1×1) to the $(\sqrt{3}\times\sqrt{3})$ phase which further evolves to the mosaic phase. Kinetic Monte Carlo (KMC) simulations allowed us to provide an explanation of experimentally obtained features using a straightforward atomistic model.

II. KMC MODEL OF DESORPTION

A solid-on-solid KMC implementation of the standard activation dynamics [14] was used for the simulations. In the model, the (111) surface is represented by a hexagonal network of adsorption sites. Atoms of two species (metal and silicon) are allowed to diffuse within this network. Only hops to unoccupied nearest positions are allowed. In addition, the metal atoms are allowed to desorb. Both diffusion and desorption processes are thermally activated. Desorption of silicon atoms is prohibited, because of much higher desorption energy, compared to the metal atoms.

For simulations we developed a code in which all possible combinations of occupations of nearest and next-nearest positions are divided into groups of configurations. Each group is associated with "configurational" energy E^c (metal and Si atoms) and with desorption energy E^{des} (metal atoms only). While E^c represents a local minimum of the surface potential, E^{des} represents directly a configuration-specific activation energy of desorption. The configurations and the corresponding energies must be defined with respect to the simulated problem while the number of configurations (ruling the number of model parameters) must be kept as low as possible. For the studied problem we defined the following configurations, examples of which can be found in Fig. 1: (1) 1×1—at least three atoms of the same and no atom of the opposite chemical

*pavel.kocan@mff.cuni.cz

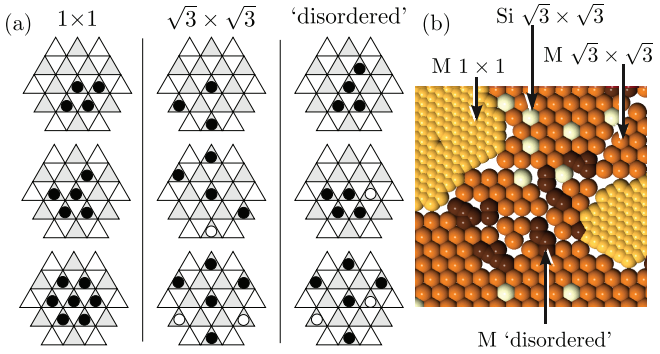

FIG. 1. (Color online) (a) Examples of configurations (with respect to the central adatom) belonging to groups named 1×1, $\sqrt{3}\times\sqrt{3}$, and "disordered" in text. The black and gray circles denote positions occupied by a metal and Si adatom. (b) Selected configurations of metal (M) and silicon (Si) atoms considered in the model are distinguished by colors (grayscale) in a simulated morphology.

species are in the nearest-neighboring positions in the 1×1 grid ($NN_{1\times1}$), forming a compact group; (2) $\sqrt{3}\times\sqrt{3}$—no atoms in $NN_{1\times1}$ and at least two atoms in nearest-neighboring positions in the $\sqrt{3}\times\sqrt{3}$ grid ($NN_{\sqrt{3}\times\sqrt{3}}$) positions; and (3) "disordered"—plain configurations not belonging to the above groups, representing atoms in transitional positions without a favorable arrangement. The group of $\sqrt{3}\times\sqrt{3}$ configurations is further divided into subgroups with respect to the number of atoms of the same chemical species in $NN_{\sqrt{3}\times\sqrt{3}}$ positions in order to allow simulation of effective repulsion in the Ising model.

The activation energy E_{act} for hopping takes into account the diffusion energy E_{dif} (corresponding to diffusion of an isolated atom) and both the initial and the final configuration energies E_i^c and E_f^c, respectively, with parabolic potentials [15],

$$E_{\mathrm{act}} = E_{\mathrm{dif}} + \frac{\Delta E}{2} + \frac{\Delta E^2}{16E_{\mathrm{dif}}}, \quad \Delta E = \left(E_i^c - E_f^c\right). \qquad (1)$$

Rates of the hopping processes are obtained as $R = \nu \exp(\frac{-E_{\mathrm{act}}}{\mathrm{k}T})$, where ν is the frequency prefactor, k is the Boltzmann constant, and T is the temperature.

An important process during mosaic phase formation is the incorporation of a substrate (Si) atom into the $\sqrt{3}\times\sqrt{3}$ structure, called substitution. As the interface between adatoms and substrate remains in plane according to STM experiments, the substituting atoms are likely to originate from step edges. The atom from the step edge may diffuse to the substituting position either *through* the adlayer by an exchange diffusion mechanism, or *on top* of the adlayer. Our simulations revealed (not shown here) that barriers allowing diffusion through the layer result in poorly ordered domains of (1×1) and $(\sqrt{3}\times\sqrt{3})$ structures, in contrast to experimental observations. On the other hand, fast diffusion on top of the adlayer results in rapid occupation of the site in the $\sqrt{3}\times\sqrt{3}$ grid after desorption of a metal atom. The fast diffusion on top of the adlayer can be awaited because the potential energy surface is smoothed by saturation of Si dangling bonds.

In order to minimize the number of model parameters, we have tested a limit case of infinite diffusion on top of the adlayer—an artificial substitution, in which an atom desorbed from the $\sqrt{3}\times\sqrt{3}$ grid is immediately (with probability of unity) replaced by a Si adatom. Both mechanisms—diffusion on top of the adlayer and the artificial substitution—give statistically the same results. Therefore, the latter is used in the simulations presented in this work.

III. RESULTS AND DISCUSSION

A. Simulations of desorption

Applicability of the model to reproduce experimentally obtained data was tested on two examples—desorption of lead and thallium from the Si(111) surface. In both cases, transition from the (1×1) to the mosaic $(\sqrt{3}\times\sqrt{3})$ phase during desorption has been observed [1,6,7,10,11].

The initial point for simulations discussed here was a complete 1×1 monolayer of the fully occupied network in the case of Pb (which is possibly a minor simplification compared to real Pb structures; see Ref. [16], and references therein). In the case of Tl we introduced experimentally obtained defects [17] within the monolayer, lowering the initial coverage to 0.97 ML.

First we will discuss the case of Pb/Si(111). The desorption spectra at constant temperatures have been published [1,9–11] using different experimental techniques: the low-energy ion-scattering spectroscopy [9], the photoemission spectroscopy [10], and the Rutherford backscattering [1,11]. Even though the data are difficult to compare quantitatively (e.g., Pb desorption rate is higher at 460 °C in Ref. [1] than at 480 °C in Ref. [10]), characteristic features are reproduced. At coverages corresponding to phase transitions, a fast change of desorption rate is observed. The desorption rate is almost constant before the transition, suggesting the ZOD. In the following, we will show that the zerolike order of desorption can be obtained as a result of the configuration-specific desorption from the surface.

In Fig. 2 we plot the simulated decrease of coverage during desorption at constant temperatures (solid lines). The desorption-related parameters used in the simulation are listed in Table I. A value of the prefactor was set to 10^{10} s^{-1}, and values of desorption energies were adjusted to correspond to

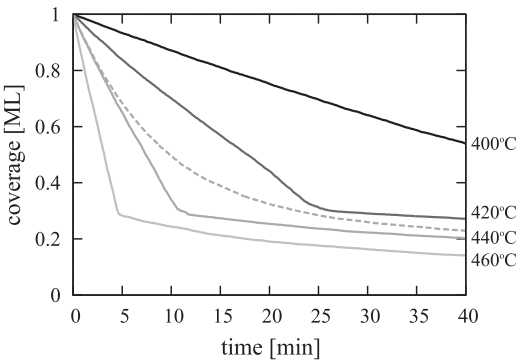

FIG. 2. Simulated isothermal desorption spectra of Pb at several temperatures. Zero-order desorption in the range 1–0.3 ML is reproduced. The dashed line is a simulated spectrum at 440 °C without enhanced desorption from disordered positions.

TABLE I. Model parameters used in simulation of Pb desorption. n denotes the number of atoms of the same chemical species in $NN_{\sqrt{3}\times\sqrt{3}}$ positions.

ν (s^{-1})	$E^{des}_{1\times1}$ (eV)	$E^{des}_{\sqrt{3}\times\sqrt{3}}$ (eV)	E^{des}_{dis} (eV)
10^{10}	1.82	$2.05 - n \times 0.025$	1.57

isothermal desorption reported in Ref. [8].[1] The overall shape is in very good agreement with experimental data [1,9–11], reproducing the fast change of the desorption rate at 0.3 ML related to $\sqrt{3}\times\sqrt{3}$ formation and an almost constant desorption rate for the coverages from 1 to 0.3 ML. The constant desorption rate at the constant temperature is an indication of an apparent ZOD. We proceed by discussing the driving force of the zerolike order of desorption. In the simulation, desorption of atoms in the disordered configuration has been enhanced by decreasing the desorption barrier from these positions by 0.25 eV compared to the 1×1 configuration (see Table I). The dashed line in Fig. 2 shows a simulated decrease of coverage at 440 °C without enhanced desorption from the disordered configurations, $E^{des}_{dis} = E^{des}_{1\times1}$. In such case, the knee at 0.3 ML disappears and almost exponential decay is obtained as in the case of the first-order desorption.

Another indication of the apparent ZOD is the characteristic sharp peak in TDS, caused by an exponential increase of the desorption rate (with temperature growing linearly) followed by a rapid drop off when all material has desorbed. The simulated TDS spectrum using the same model parameters as in Fig. 2 is shown in Fig. 3 by the black solid line, clearly showing the ZOD features. The exponential part is fitted by the theoretical dependence (red dashed line) with parameter $E_{eff} = 1.78$ eV. The desorption rate of atoms in the disordered configurations is plotted by the blue dash-dotted line in Fig. 3. It is evident that the desorption rate of these atoms increases during the structural transition and vanishes when the surface reaches coverage allowing incorporation of all atoms in a stable structure (in our case the $\sqrt{3}\times\sqrt{3}$). In other words, an enhanced desorption of atoms in disordered configuration is responsible for the ZOD behavior in our model.

Snapshots of the morphologies obtained by the simulation of the desorption at 460 °C are shown in Fig. 4. Two phases can be found on the snapshots corresponding to $\sim 2/3$ of ML [Fig. 4(a)]: the "smooth" 1×1 coexisting with islands of the $\sqrt{3}\times\sqrt{3}$ phase. Several Pb atoms (light balls) in the $\sqrt{3}\times\sqrt{3}$ structure are substituted by Si atoms (dark balls). Figure 4(b) shows the surface with $\sim 1/3$ of Pb ML, completely reconstructed to the $\sqrt{3}\times\sqrt{3}$ phase. A small fraction of substituted atoms can be found. After further desorption, this fraction increases, resulting in the $\sqrt{3}\times\sqrt{3}$ mosaic phase at $\sim 1/6$ ML coverage.

[1]Please note that exact fitting of experimental data was not the aim, since desorption characteristics [1,9–11] do not coincide together due to different techniques used. Because of the rather small range of temperatures allowing reasonable observation of desorption, an impact of the prefactor value is rather small, in other words, after adjusting desorption energies different values of prefactors could be used as well.

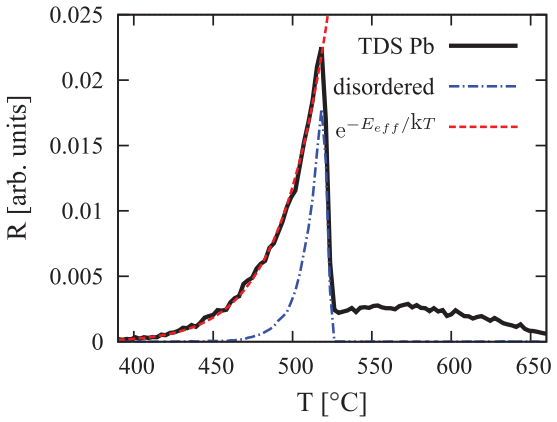

FIG. 3. (Color online) Simulated thermal desorption spectrum of Pb, temperature increasing with rate 1 K s^{-1}. Black solid line, total desorption flux; red dashed line, exponential fit; blue dash-dotted line, desorption flux corresponding to desorption from disordered positions.

In the case of desorption of thallium from the Si(111) surface, a different kind of experimental data is available [7]. In Fig. 5, Tl coverages obtained from STM morphologies after 2 min of desorption at various temperatures are plotted by squares. Contrary to Pb desorption case, the $\sqrt{3}\times\sqrt{3}$ structure without substitutional Si atoms has not been observed. Instead, the mosaic phase is formed immediately from the 1×1 phase by desorption. Previously we have demonstrated that the observed desorption characteristics can be explained using a single desorption energy in all adsorption positions, and the values $E_{des} = (2.1 \pm 0.3)$ eV, $\nu = 5 \times 10^{14\pm2}$ s^{-1} were obtained by fitting [7]. Results of the simulation using the same parameters are plotted in Fig. 5 by the solid line. Not surprisingly, good agreement is obtained, since KMC and rate equations (Ref. [7]) are solutions of the same problem. The advantage of KMC simulations is that morphologies of simulated and experimental data can be directly compared. The simulated morphologies of layers after 120 s of desorption at 300 °C, 330 °C, and 350 °C are shown in Fig. 6. Compared to the STM data [7] a nice agreement is obtained. At a temperature of 300 °C corresponding to the desorption onset, only small islands of the originating $\sqrt{3}\times\sqrt{3}$ structure are formed [Fig. 6(a)]. By the desorption at 330 °C [Fig. 6(b)], islands of $\sqrt{3}\times\sqrt{3}$ structure are formed. A significant amount

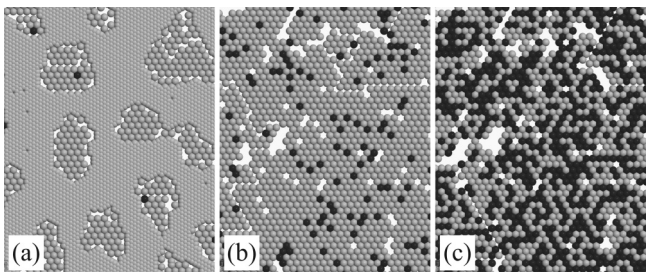

FIG. 4. Snapshots of simulated Pb morphologies during desorption from the initial 1×1 structure at 460 °C. light (dark) gray balls represent Pb (Si) atoms. (a) $\sim 2/3$ ML, coexisting 1×1 and $\sqrt{3}\times\sqrt{3}$ structures. (b) $\sim 1/3$ ML, $\sqrt{3}\times\sqrt{3}$ with several substituted atoms. (c) $\sim 1/6$ ML, mosaic $\sqrt{3}\times\sqrt{3}$ phase.

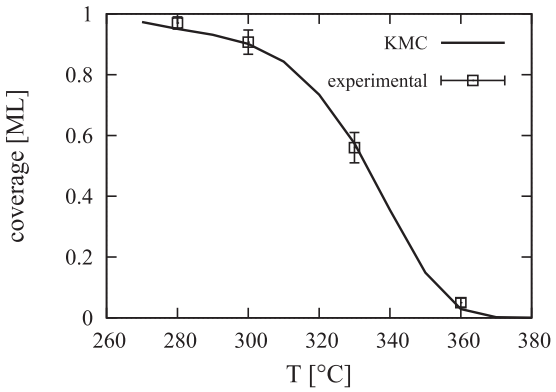

FIG. 5. Residual Tl coverage after 120 s of desorption as a function of temperature. Experimental data (squares) are taken from Ref. [7]; the simulated curve was obtained using the desorption rate independent on atomic configurations.

of Si substitutional atoms in the $\sqrt{3}\times\sqrt{3}$ structure is caused by the same probability of desorption from all structures, in agreement with experiments. The desorption at 350 °C results in the surface being completely covered by the $\sqrt{3}\times\sqrt{3}$ mosaic phase, as shown in Fig. 6(c).

A TDS curve calculated for Tl desorption (plotted in Fig. 7 by the black solid line) has clearly a first-order character. The green dashed, red dotted, and blue dash-dotted lines show desorption from 1×1, $\sqrt{3}\times\sqrt{3}$, and disordered configurations, respectively. The contribution of the disordered configuration reaches maximum when amounts of atoms in dense and sparse structures are comparable.

B. Simulations of the mosaic phase ordering

Ordering of the $\sqrt{3}\times\sqrt{3}$ mosaic phases has been studied in several works as an example of a 2D antiferromagnetic Ising system with the hexagonal symmetry [2,5,18]. In the case of the 1 : 1 ratio of metal and substitutional atoms, the highly degenerated ground state of the system is represented by an infinite number of configurations with two same-element nearest neighbors (SENNs) on average [5]. A geometric frustration, caused by impossibility to reach zero SENNs on average, results in only local ordering. Previously, the ordering has been studied by means of Monte Carlo simulations using a nonrealistic dynamics based on an exchange of atoms in neighboring $\sqrt{3}\times\sqrt{3}$ positions [5].

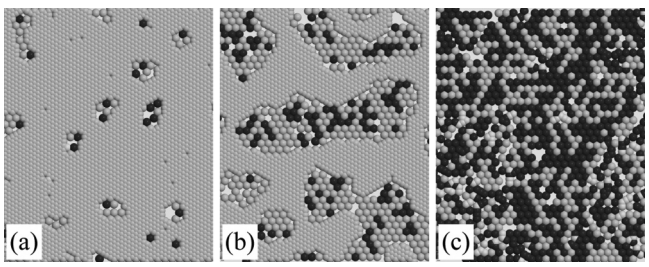

FIG. 6. Snapshots of simulated Tl morphologies obtained after 120 s of desorption at (a) 300 °C, (b) 330 °C, and (c) 350 °C. Light (dark) gray balls represent Tl (Si) atoms.

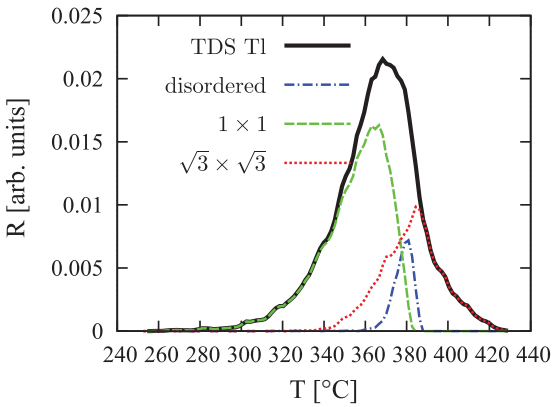

FIG. 7. (Color online) Simulated thermal desorption spectrum of Tl (black solid line), temperature increasing with rate 1 K s^{-1}. Green dashed, red dotted, and blue dash-dotted lines show desorption from 1×1, $\sqrt{3}\times\sqrt{3}$, and disordered configurations.

Since our model is based on hopping within the 1×1 network, an exchange of neighboring atoms can be realized in a close-to-realistic way and probability of the exchange can be tested. Considering in-plane hopping limited to the 1×1 network, the process itself consists of several steps, as depicted in Fig. 8: (1) hopping of an adatom out of a stable $\sqrt{3}\times\sqrt{3}$ position "A" to a first transitional position "B," (2) a neighboring atom leaving its position, resulting in the second transitional configuration "C," and (3) hops of atoms to final positions "D." The schematic energy potential profile of the exchange is shown on the right-hand side in Fig. 8. Since the activation energies of hops are calculated using Eq. (1), the barrier of hopping from the stable $\sqrt{3}\times\sqrt{3}$ position to the transitional position (A to B) is high. Moreover, to realize an exchange, two such events must appear concertedly before the atom collapses to the initial position. The energy barrier for such collapse (B to A) is small. Therefore, in the frame of our model, a direct exchange can be supposed to be very rare. Our simulations of the surface covered by 1/6 of Pb ML and 1/6 of Si ML with the prohibited desorption revealed that if E_{dif} in Eq. (1) is sufficiently low (otherwise no changes are observed), rather whole domains of surface rearrange instead of a pairwise exchange of atoms. Introducing diffusing vacancies [19] facilitates and speeds up kinetics of the system. However, the obtained morphologies are less ordered (average number of nearest neighbors of the same species is higher) than those observed experimentally [2,5]. The reason is probably related to a high level of system frustration [20].

In order to provide a mechanism of the observed local mosaic ordering, we have tested a model utilizing a selective

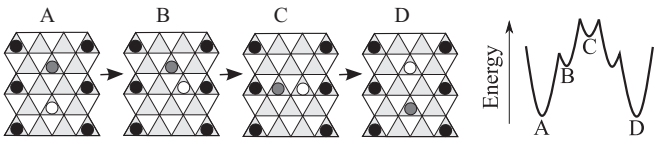

FIG. 8. Step-by-step exchange of two atoms (white and gray circle) in the $\sqrt{3}\times\sqrt{3}$ network via the 1×1 grid. Right-hand side: A schematic potential profile along the kinetic pathway of the exchange. A–D mark local potential minima and corresponding configurations.

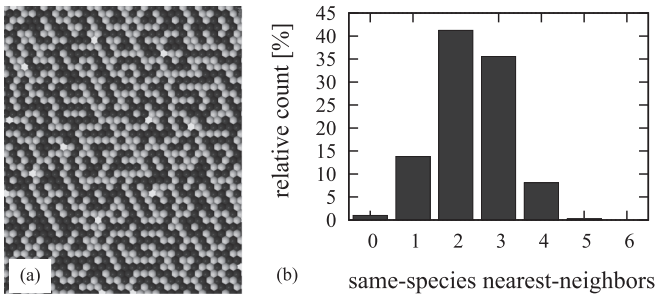

FIG. 9. (a) Simulated morphology of the mosaic phase (1 : 1 ratio Pb : Si) formed by desorption from the $\sqrt{3}\times\sqrt{3}$ phase with 1/3 ML of Pb atoms, with prohibited diffusion. (b) A histogram of the same-species nearest-neighbors occupancy.

desorption. In this model, the desorption energy depends linearly on the number of same-species nearest neighbors. In the simulations further discussed, we started from the $\sqrt{3}\times\sqrt{3}$ lattice fully occupied by metal atoms. During the simulations, events of desorption with the artificial substitution by Si atoms were generated. Hopping of atoms was suppressed in the simulations in order to separate diffusion and desorption effects. Figure 9(a) shows the simulated morphology corresponding to the 1 : 1 ratio of metal and Si atoms. The desorption energy was calculated as $E^{\mathrm{des}}_{\sqrt{3}\times\sqrt{3}} = (2.05\,\mathrm{eV} - NN^{\mathrm{SE}}_{\sqrt{3}\times\sqrt{3}} \times \Delta E_{\mathrm{des}})$, where $NN^{\mathrm{SE}}_{\sqrt{3}\times\sqrt{3}}$ denotes a number of same-species nearest neighbors in the $\sqrt{3}\times\sqrt{3}$ grid. Since we select the structure corresponding to the 1 : 1 ratio of metal and Si atoms, the only important parameter is $\Delta E_{\mathrm{des}}/kT$. At the given temperature of 530 °C [21], the best agreement with the morphology published in Ref. [2] was obtained for a value $\Delta E_{\mathrm{des}} = (0.09 \pm 0.03)$ eV. A histogram of the same-species nearest neighbors calculated from the morphology obtained under such conditions is shown in Fig. 9(b) and a nice agreement is obtained with the morphologies observed experimentally [2].

A rough estimate of the value of ΔE_{des} can be obtained from Ref. [2], where the total energies E_{tot} of selected mosaic configurations of Pb and Si atoms with the 1 : 1 ratio are calculated using the density functional theory. Assuming E_{tot} can be separated to the bonding energy to the substrate (the same in all studied cases) and to the energy of adatom-adatom interactions, the repulsive term ΔE_{tot} can be estimated from the slope of the dependence of E_{tot} on the number of same-element neighbors in the structure [21]. By this procedure, a value $\Delta E_{\mathrm{tot}} = (0.12 \pm 0.02)$ eV per pair is obtained, which is close to the value used in our simulations.

The above result demonstrates that local ordering can be achieved without exchange or diffusion processes, solely as a consequence of the selective desorption and substitution. However, we note that under experimental conditions the diffusion cannot be ruled out at elevated temperatures, at which the mosaic structures are formed. In such case, both the desorption and the diffusion are likely to influence the level of ordering.

IV. CONCLUSIONS

A configuration-based KMC model of desorption-induced structural transitions was used to reproduce experimentally observed morphologies. We have demonstrated that the selective desorption can explain two important features. First, the zero-order-like desorption observed in several cases can be obtained as a result of lower desorption energy of atoms in disordered configurations. Concentration of these atoms increases during the transition from the 1×1 to the $\sqrt{3}\times\sqrt{3}$ phase. Second, a local ordering of the mosaic $\sqrt{3}\times\sqrt{3}$ phase can be achieved by setting the activation energy of the substitution linearly dependent on the number of the same-element nearest neighbors.

[1] E. Ganz, F. Xiong, I. S. Hwang, and J. Golovchenko, Phys. Rev. B **43**, 7316 (1991).
[2] M. Švec, P. Jelínek, P. Shukrynau, C. González, V. Cháb, and V. Drchal, Phys. Rev. B **77**, 125104 (2008).
[3] B. Ressel, J. Slezák, K. C. Prince, and V. Cháb, Phys. Rev. B **66**, 035325 (2002).
[4] C. Törnevik, M. Göthelid, M. Hammar, U. Karlsson, N. Nilsson, S. Flodström, C. Wigren, and M. Östling, Surf. Sci. **314**, 179 (1994).
[5] L. Ottaviano, B. Ressel, C. Di Teodoro, G. Profeta, S. Santucci, V. Cháb, and K. C. Prince, Phys. Rev. B **67**, 045401 (2003).
[6] V. G. Kotlyar, A. A. Saranin, A. V. Zotov, and T. V. Kasyanova, Surf. Sci. **543**, L663 (2003).
[7] P. Kocán, P. Sobotík, P. Matvija, M. Setvín, and I. Ošt'ádal, Surf. Sci. **606**, 991 (2012).
[8] N. Minami, Y. Machida, T. Kajikawa, T. Sato, K. Ota, and S. Ino, Surf. Sci. **524**, 199 (2003).
[9] M. Saitoh, K. Oura, K. Asano, F. Shoji, and T. Hanawa, Surf. Sci. **154**, 394 (1985).
[10] J. A. Carlisle, T. Miller, and T. C. Chiang, Phys. Rev. B **45**, 3400 (1992).
[11] E. Ganz, H. Shouh, X. Fulin, S. Theiss, and J. Golovchenko, Surf. Sci. **257**, 259 (1991).
[12] S. King, R. Davis, and R. Nemanich, Surf. Sci. **602**, 405 (2008).
[13] H. Kreuzer and S. Payne, Surf. Sci. **200**, L433 (1988).
[14] C. Ratsch and J. A. Venables, J. Vac. Sci. Technol. A **21**, S96 (2003).
[15] E. S. Hood, B. H. Toby, and W. H. Weinberg, Phys. Rev. Lett. **55**, 2437 (1985).
[16] S. C. Jung and M. H. Kang, Phys. Rev. B **84**, 155422 (2011).
[17] P. Kocán, P. Sobotík, and I. Ošt'ádal, Phys. Rev. B **84**, 233304 (2011).
[18] J. M. Carpinelli, H. H. Weitering, and E. Plummer, Surf. Sci. **401**, L457 (1998).
[19] E. Vives and A. Planes, Phys. Rev. B **47**, 2557 (1993).
[20] G. H. Wannier, Phys. Rev. **79**, 357 (1950).
[21] M. Švec (private communication).